XUV frequency comb spectroscopy

Gohle, C.; Kandula, D.Z.; Pinkert, T.J.; Ubachs, W.M.G.; Eikema, K.S.E.

published in
Proceedings of the XIX International Conference on Laser Spectroscopy
2010

XUV FREQUENCY COMB SPECTROSCOPY

C. GOHLE, D. Z. KANDULA, T. J. PINKERT, W. UBACHS, and K.S.E. EIKEMA*

Laser Centre, Vrije Universiteit,
De Boelelaan 1081, 1081 HV, Amsterdam, The Netherlands
**E-mail: KSE.Eikema@few.vu.nl*

Frequency comb lasers in the infrared region of the spectrum have revolutionized many fields of physics. We demonstrate for the first time direct frequency comb spectroscopy at XUV wavelengths. Generation of an XUV comb is realized by amplification of two pulses from a frequency comb laser in a parametric amplifier, and subsequent high-harmonic generation to 51 nm (15^{th} harmonic). These XUV pulses, with a time separation between 5.4 and 10 ns, are then used to directly excite helium on the $1s^2\ ^1S_0$ – $1s5p\ ^1P_1$ transition. The resulting Ramsey-like signal has up to 60% modulation contrast, indicating a high phase coherence of the generated XUV comb light.

Keywords: Frequency combs; Spectroscopy; Extreme Ultraviolet; Helium;

1. Introduction

The invention of the self-referenced frequency comb laser[1,2] has caused a revolution in precision frequency metrology and attosecond laser science (see e.g. [3,4]). Comb lasers are based on a mode-locked (ultrafast) laser, emitting pulses that have a precisely controlled timing and phase. Because of the Fourier-relation between time-and frequency domain, this results in a spectrum consisting of modes that have frequencies that are completely determined by just three numbers: the mode number n, the repetition rate of the pulses f_{rep}, and an offset frequency f_0 (see Fig. 1). Both f_{rep} and f_0 are in the radio-frequency domain and can be locked and calibrated with high precision against an atomic reference. The mode spacing f_{rep} is equal to the inverse time T between two pulses ($f_{rep} = 1/T$). Likewise, the carrier-envelope phase shift $\Delta\phi_{CE}$ of the pulses corresponds to an offset frequency of the 'comb-like' spectrum according to $\Delta\phi_{CE} = 2\pi f_0/f_{rep}$. For each mode we can write:

$$f_n = f_{ceo} + n f_{rep} \tag{1}$$

A common use of comb lasers is spectroscopic calibration by measuring a beat note between the comb modes and a narrow-bandwidth laser used for spectroscopy. This is routinely performed in the (near) infrared, as most comb lasers are based on Ti:Sapphire or fiber modelocked lasers. Spectral coverage can be extended via nonlinear interaction in photonic fibers, and particularly to short wavelengths by harmonic generation. So far, comb generation has been verified down to vacuum ultraviolet (VUV) radiation (see e.g. [5–9]).

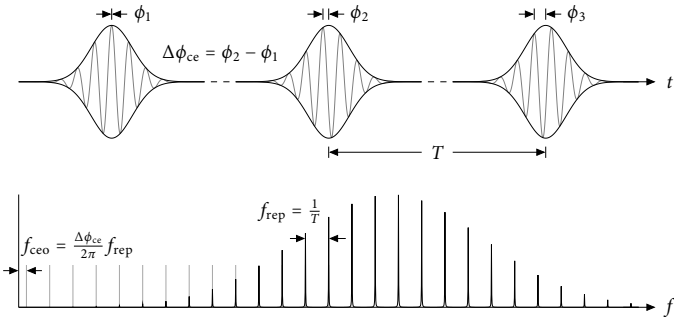

Fig. 1. The frequency comb laser principle based on a mode locked laser. Upper half: time domain representation as phase-coherent laser pulses. Lower half: frequency domain representation in the form of resonator modes, parameterized with f_{rep} (repetition frequency) and f_{ceo} (the carrier-envelope offset frequency).

Extending frequency comb lasers further to the extreme ultraviolet (XUV) is of interest for e.g. precision measurements in neutral helium atoms and hydrogen-like helium$^+$ ions. These systems can provide interesting tests of one- and two-electron QED effects, especially if excited from the ground state where QED influences are an order of magnitude stronger than in the exited states (for a theoretical treatment see e.g.[10–12]). However, frequency comb spectroscopy at extreme ultraviolet (XUV) wavelengths has not been demonstrated up to now. Here we show how this can be accomplished using amplification and up-conversion of frequency comb pulses.

2. Principle of direct frequency comb excitation in the XUV

To extend comb lasers to the XUV, the high peak power of the comb pulses can be exploited to generate high-harmonics. Theoretically [13–15] and experimentally [14,15] it has been shown that high-harmonic generation (HHG) can result in phase coherent XUV pulses, which is a prerequisite of frequency comb generation in the XUV. However, it was unclear so far, if the comb structure would survive the HHG process as the phase relation between driving pulses and XUV pulses could be time varying. Nevertheless, with enough peak power in the comb laser pulses (either by amplification,[7,8,16] or enhancement in an optical resonator[5,6]), it is possible to generate light with wavelengths well into the XUV. If the phase relation between the pulses is controlled better than a small fraction of an optical cycle, the spectrum of the newly generated light should show a similar subdivision in comb modes as the fundamental light.

Each of the modes of a (upconverted) frequency comb can be regarded as a continous wave (CW) laser and therefore be used for high resolution spectroscopy. This is especially useful in the XUV domain, where no real narrowband CW sources are available. Additionally, this direct frequency comb spectroscopy (DFCS) combines excitation and calibration which simplifies the spectroscopic procedure. The principle of excitation with phase coher-

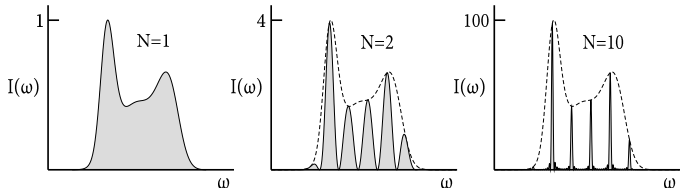

Fig. 2. Relation between the number of phase coherent pulses N (with a fixed phase difference), and the resulting spectrum in the frequency domain.

ent pulses[17] is very similar to Ramsey spectroscopy with spatially separated fields.[18] Experimentally it was already explored in the late 1970's[19,20] by exciting atomic sodium using dye laser pulses in a resonator. Because f_0 control was not possible at that time, only frequency differences within the bandwidth of the laser could be measured. With the invention of the frequency comb laser the situation has changed, making DFCS a very interesting new tool for spectroscopy (see e.g. [7,8,21]).

Converting frequency combs to VUV and XUV wavelengths by focusing in a gas jet requires a peak intensity on the order of 10^{13} W/cm^2 to 10^{14} W/cm^2. Typical comb laser output pulse energies are in the nJ range, which is not enough. The solution chosen in our lab is based on amplification of only a few subsequent pulses from a comb laser. Pulse energies of tens of μJ,[7,8] and even mJ level[16] have been reached for pairs of subsequent comb pulses, sufficient for HHG. By amplification and up-conversion of subsequent pulses one can retain the mode spacing of the original comb, but the spectral shape of the 'modes' change. In Fig. 2 the comb mode shape is shown for 1, 2 and 10 pulses. It can be seen that 2 pulses already contain the essential information of the comb line positions, but that the mode structure resembles a cosine modulated spectrum. The idea is then to amplify two comb pulses, and convert them to XUV via harmonic generation. The spectrum of the XUV pulses will also look like a cosine-'frequency comb', which is then used to directly excite helium.

3. Experiment: amplification of frequency comb pulses

For our approach, pulses from a comb laser have to be amplified and the phase distortion characterized. In Fig. 3 a schematic is shown of this part of the experimental setup. A Ti:Sapphire frequency comb with f_{rep} tunable from 100–185 MHz serves as a source of phase-controlled pulses with a central wavelength of 773 nm. This is followed by a dedicated optical parametric amplifier (OPA) based on 2 BBO crystals. The parametric amplification process is driven by a pulse-pair of 532 nm from a pump laser, so that two subsequent pulses from the comb laser can be amplified to a few mJ per pulse. Parametric amplification has several advantages over traditional Ti:sapphire amplification, including a wide amplification bandwidth (700–1000 nm). The fact that no energy is dissipated in the crystals implies that there is no memory effect between the two amplified pulses.

Because harmonic up-conversion is used to create an XUV frequency comb, its f_0 is higher than the original f_0 with the same factor as the harmonic order (f_{rep} is not changed). Any phase distortion due to the amplification process is multiplied with the harmonic order as well. Therefore the phase control should be accurate to about 20 mrad or less in the infrared, if the 15$^{\text{th}}$ harmonic is used. This requirement must be met for the whole spatial beam profile of the amplified beam. Inspection of the parametric amplification process reveals that a small additional phase is imparted on the signal beam due to a phase-mismatch ($\Delta k = k_p - k_s - k_i$ between the k-vectors involved (denoted as k_p, k_s, k_i respectively for pump, signal and

idler photon). The phase shift due to the parametric process is given by the product of Δk and a pump-depletion integral.[16,22] It can easily exceed several hundred mrad. Therefore significant effort was made to in the design of the pump laser and to measure of the phase distortions in the parametric amplification process accurately.

The pump laser consists of a commercial modelocked Nd:YVO_4 oscillator (High-Q laser), operating at 1064 nm. It produces 7 ps pulses at 70 MHz repetition rate with an average power of 3W. The pulsetrain is electronically synchronized to the comb laser by feeding back onto the laser cavity length. After a reduction in spectral bandwidth, the pulses are amplified in a regenerative amplifier based on a laserdiode-pumped Nd:YAG module. This results in pulses of 2 mJ and 50 ps at a repetition rate of 28 Hz. At this point the pulses are split in two, using polarizing optics and a delay line of several meters in length. After the delay line the pulses are combined again to continue along the same optical path again. As a result, 2 pump pulses are generated at a time delay equal to the comb pulse delay. Special care is taken to keep the wavefront of the two pulses equal by employing relay-imaging and 2 vertical periscopes (as relay-imaging reverses up-down and left-right). The pulses (typically 5.4–10 ns apart for a comb repetition rate frequency of 185 MHz – 100 MHz) are subsequently amplified further in two flashlamp-pumped Nd:YAG amplifier units. Equal energy pump pulses of 200 mJ each are obtained at the output of this stage after adjusting the splitting ratio at the delay line appropriately.

The parametric amplifier itself is based on two BBO crystals. Both crystals are pumped with 532 nm radiation obtained by frequency doubling the pulses from the pump laser. In order to amplify two pulses from the comb laser, the comb pulses are stretched in time with a grating-based stretcher, which includes a slit as well to reduce the bandwidth of the pulses to 6 nm. These pulses are then amplified in the first crystal using a double-pass geometry, and spatially filtered with a pinhole. After increasing the beam diameter to about 6 mm, the beam is amplified to a level of 5 mJ per pulse in the second crystal. Compression in a grating compressor results in pulses of 200 fs duration with approximately 2.5 mJ per pulse.

Self-phase or cross-phase modulation can also result in spatially dependent phase errors due to an inhomogeneous intensity in the (pump)beam. To minimize these effects, a spatial filter with ceramic pinhole (sitting in vacuum) is used (diameter 0.08 mm, typical throughput $\leq$75%) to filter out all higher order mode contributions in the beam. The spatial filtering also reduces possible wavefront errors between the two pulses.

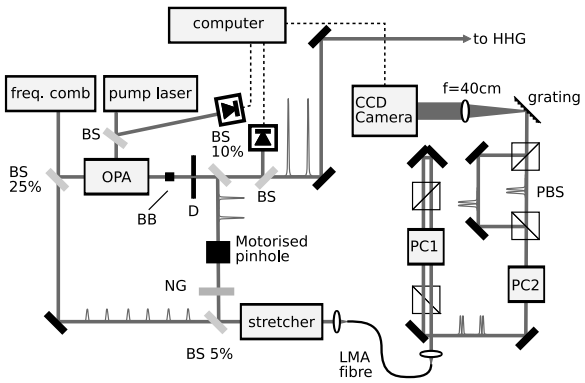

Fig. 3. Experimental setup for frequency comb amplification and phase characterization. OPA=optical parametric amplifier, NG=neutral gray filter, BB=beam block, BS=beam splitter, D=iris, LMA=large-mode area photonic fiber, PC1,2=Pockels-cell

4. Phase characterization of the amplified comb pulses

To investigate phase distortions due to the OPA, we use an interferometric measurement technique (see Fig. 3). To this end, a Mach-Zehnder interferometer is built by splitting off part of the frequency comb signal before the parametric amplifier and recombining it with a small part of the amplified signal. It is followed by a grating-stretcher and a large-mode volume photonic fiber (20 μm mode field diameter, from Crystal Fibre) to ensure that possible self-phase modulation is suppressed and both amplified and reference beams are in exactly the same mode. A Pockels-cell (PC1 in Fig. 3) is used to block references pulses that do not belong to the amplified pulse pair.

The phase of the pulses can vary for each laser shot, therefore we employ spectral interferometry, which allows to determine the phase single-shot. For this purpose a small time delay ($\approx$1 ps) is applied between the amplified and reference pulses, leading to a wavelength dependent interference pattern that can be measured using a spectrometer. The spectrometer consists of a 1200 l/mm grating, a f=40 cm imaging lens, and a gated CCD camera. A second Pockels cell (PC2) is used with polarizing optics to switch between the two amplified pulses and direct the corresponding interferograms to spatially separate regions on the camera. The differential phase shift between the two amplified pulses is then obtained determining the fringe pattern position difference, while periodically swapping the two interferograms to eliminate geometric differences. Tests have shown that the

method is accurate to better than 5 mrad and a rms single shot noise of 10 mrad.

With the procedure explained above, a phase shift is measured for each laser shot averaged over the entire beam profile (or the normal mode that is matched to the fiber mode). However, this phase shift can be spatially dependent. This dependence cannot be measured for each laser pulse, but it is typically stable enough so that the spatial phase dependence can be measured just before recording a helium signal. To accommodate for this, and to separate the XUV from the infrared driving field later in the setup, the amplified laser beam is converted into an annular mode (by a beam-block, leaving a shadow of 2 mm in the center of the 6 mm wide beam). An automated pinhole is used to scan across the annular mode in order to map out the phase differences between the two laser pulses as a function of the pinhole position. Typically a spatial dependence is found on the order of 30 mrad rms and typically corresponds to a wavefront tilt.

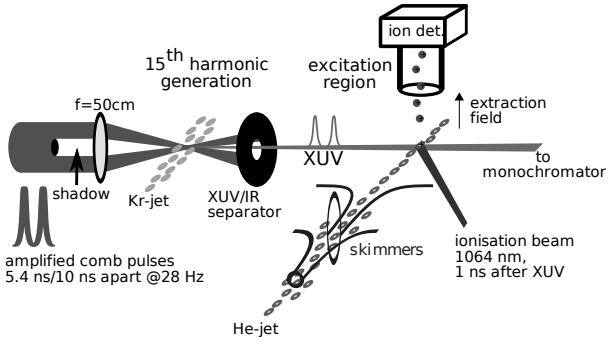

Fig. 4. High-harmonic generation and helium excitation setup

5. Results: XUV comb generation and excitation of helium

For harmonic up conversion ≈1–1.5 mJ (per pulse in a donut mode) is focused in a pulsed krypton jet. About 10^8 photons are generated per pulse at the 15^{th} harmonic (average power 10 nW). Because two pulses are converted, a cosine-like comb in the XUV is generated. After the harmonic conversion, the beam encounters a pinhole that separates the HHG light, in the center of the beam, from the high power infrared donut mode (see Fig. 4). Helium is subsequently excited on the $1s^2\ ^1S_0 - 1s5p\ ^1P_1$ transition

using a crossed atomic beam setup, where skimmers and seeding in heavier noble gasses are used to reduce Doppler broadening and shifts. A simplified excitation scheme is shown in Fig. 5.

After excitation with an XUV pulse pair, a pulse at 1064 nm is used to ionize the excited atoms. Only atoms excited to 4p and higher are ionized by the infrared laser. The spectral width of the XUV pulse, and the conditions in the harmonic generation are chosen such that only one level is excited by the XUV light from one harmonic. Direct ionization by the 17th harmonic results in only 10% constant background counts, while the 13th harmonic 2p contribution is not ionized by the 1064 nm pulse. The bandwidth of the 15th harmonic is verified to be small enough to have less than 1% excitation of the neighboring (4p and 6p) transitions. A spectrum is recorded by counting the ion yield while varying the pulse distance. Each scan takes about 15 minutes, and the pulse delay is changed in steps of 1 attosecond by adjusting f_{rep}. After binning the data into about 50 frequency bins, a Ramsey-like excitation spectrum emerges as shown in Fig. 6.

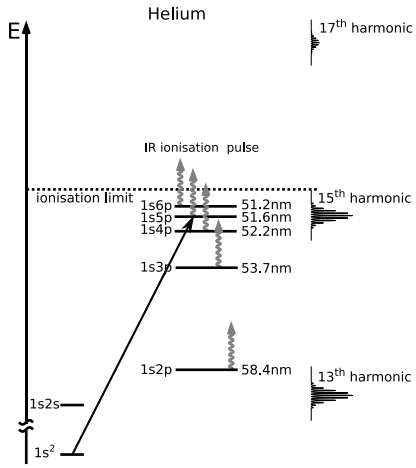

Fig. 5. XUV excitation scheme in neutral helium. The thick wavy arrows indicate the ionization laser at 1064 nm. Note that the spectral width of the harmonic orders is exaggerated, and the number of 'cosine modes' reduced, for better visibility.

A mixture of neon and helium was used (5:1) in this example to reduce Doppler broadening. The best contrast of 60% of the recorded cosine-modes have been obtained using a f_{rep}=184 MHz and a helium-argon mixture.

To achieve an absolute calibration for the transition, many systematic

effects have been investigated. Apart from the phase shifts in the OPA, this includes e.g. Doppler-shifts, DC and AC Stark shifts, Zeeman shift, chirp, pulse ratio (which primarily tests the adiabatic phase shift in the harmonic generation), pulse intensity, and many more. The pulse distance was also varied from 5.4 ns to 10 ns, to identify the comb mode that was used for the excitation.

At the time of writing the analysis of all systematic effects has not been fully completed, therefore no absolute number is given here for the ground state energy of helium. However, a preliminary estimation shows that an accuracy of better than 10 MHz is realistic for the current experiment, which would already be a 5 fold improvement over results obtained without frequency combs.[23,24]

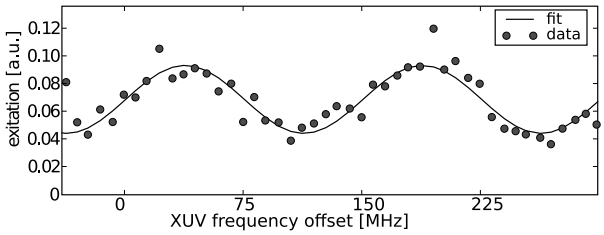

Fig. 6. Direct XUV comb excitation ion signal on the helium $1s^2\ ^1S_0$ – $1s5p\ ^1P_1$ transition at 51.6 nm, where f_{rep}=148 MHz, and a mixture of helium and neon was used. The zero of the frequency axis is based on theoretical level energies from Ref.[10]

6. Conclusions and outlook

For the first time high-resolution XUV frequency comb spectroscopy has been demonstrated, and an accuracy has been reached on the 10 MHz level. Further progress is expected for a bigger delay time between the pulses as the accuracy is inversely proportional to the pulse delay. Given the phase coherence seen at the 15^{th} harmonic, it is conceivable to extend the range of XUV comb spectroscopy to much shorter wavelengths and excite e.g. helium$^+$ ions.

Acknowledgments

This work was supported by the Foundation for Fundamental Research on Matter (FOM), the Dutch Science Organization (NWO), Laserlab Europe (JRA Aladin), and the Humboldt Foundation.

References

1. R. Holzwarth, T. Udem, T. W. Hänsch, J. C. Knight, W. J. Wadsworth and P. S. J. Russell, *Phys. Rev. Lett.* **85**, 2264 (2000).
2. D. Jones, S. Diddams, J. Ranka, A. Stentz, R. Windeler, J. Hall and S. Cundiff, *Science* **288**, 635(APR 28 2000).
3. P. B. Corkum and F. Krausz, *Nature Physics* **3**, 381(JUN 2007).
4. A. Baltuska, T. Udem, M. Uiberacker, M. Hentschel, E. Goulielmakis, C. Gohle, R. Holzwarth, V. Yakoviev, A. Scrinzi, T. Hansch and F. Krausz, *Nature* **421**, 611(FEB 6 2003).
5. C. Gohle, T. Udem, M. Herrmann, J. Rauschenberger, R. Holzwarth, H. A. Schuessler, F. Krausz and T. W. Hänsch, *Nature* **436**, 234(July 2005).
6. R. J. Jones, K. D. Moll, M. J. Thorpe and J. Ye, *Phys. Rev. Lett.* **94**, p. 193201 (2005).
7. S. Witte, R. Zinkstok, W. Ubachs, W. Hogervorst and K. Eikema, *Science* **307**, 400(JAN 21 2005).
8. R. T. Zinkstok, S. Witte, W. Ubachs, W. Hogervorst and K. S. E. Eikema, *Phys. Rev. A* **73**, p. 061801(R) (2006).
9. A. L. Wolf, S. A. van den Berg, W. Ubachs and K. S. E. Eikema, *Phys. Rev. Lett.* **102**(JUN 5 2009).
10. G. W. F. Drake and Z.-C. Yan, *Can. J. Phys.* **86**, 45(JAN 2008).
11. K. Pachucki, *Phys. Rev. A* **76**, p. 059906(NOV 2007).
12. S. Karshenboim, *Phys. Rep.* **422**, 1(DEC 2005).
13. M. Lewenstein, P. Salieres and A. Lhuillier, *Phys. Rev. A* **52**, 4747(DEC 1995).
14. R. Zerne, C. Altucci, M. Bellini, M. B. Gaarde, T. W. Hänsch, A. L'Huillier, C. Lyngå and C.-G. Wahlström, *Phys. Rev. Lett.* **79**, 1006 (1997).
15. S. Cavalieri, R. Eramo, M. Materazzi, C. Corsi and M. Bellini, *Phys. Rev. Lett.* **89**, p. 133002 (2002).
16. D. Z. Kandula, A. Renault, C. Gohle, A. L. Wolf, S. Witte, W. Hogervorst, W. Ubachs and K. S. E. Eikema, *Opt. Express* **16**, 7071(MAY 12 2008).
17. Y. V. Baklanov and V. P. Chebotaev, *Appl. Phys. A* **12**, 97 (1977).
18. N. F. Ramsey, *Phys. Rev.* **76**, 996(Oct 1949).
19. R. Teets, J. Eckstein and T. W. Hänsch, *Phys. Rev. Lett.* **38**, 760(Apr 1977).
20. J. N. Eckstein, A. I. Ferguson and T. W. Hänsch, *Phys. Rev. Lett.* **40**, 847(Mar 1978).
21. A. Marian, M. Stowe, J. Lawall, D. Felinto and J. Ye, *Science* **306**, 2063(DEC 17 2004).
22. A. Renault, D. Z. Kandula, S. Witte, A. L. Wolf, R. T. Zinkstok, W. Hogervorst and K. S. E. Eikema, *Opt. Lett.* **32**, 2363(AUG 15 2007).
23. K. S. E. Eikema, W. Ubachs, W. Vassen and W. Hogervorst, *Phys. Rev. A* **55**, 1866(Mar 1997).
24. S. D. Bergeson, A. Balakrishnan, K. G. H. Baldwin, T. B. Lucatorto, J. P. Marangos, T. J. McIlrath, T. R. O'Brian, S. L. Rolston, C. J. Sansonetti, J. Wen, N. Westbrook, C. H. Cheng and E. E. Eyler, *Phys. Rev. Lett.* **80**, 3475(Apr 1998).